Programmed fluctuations in sense/antisense transcript ratios drive sexual differentiation in *S. pombe*

Danny A. Bitton, Agnes Grallert, Paul J. Scutt, Tim Yates, Yaoyong Li, James R. Bradford, Yvonne Hey, Stuart D. Pepper, Iain M. Hagan, Crispin J. Miller

Supplementary Figures S1-13 and supplementary Tables S1, S3, S8 and S11

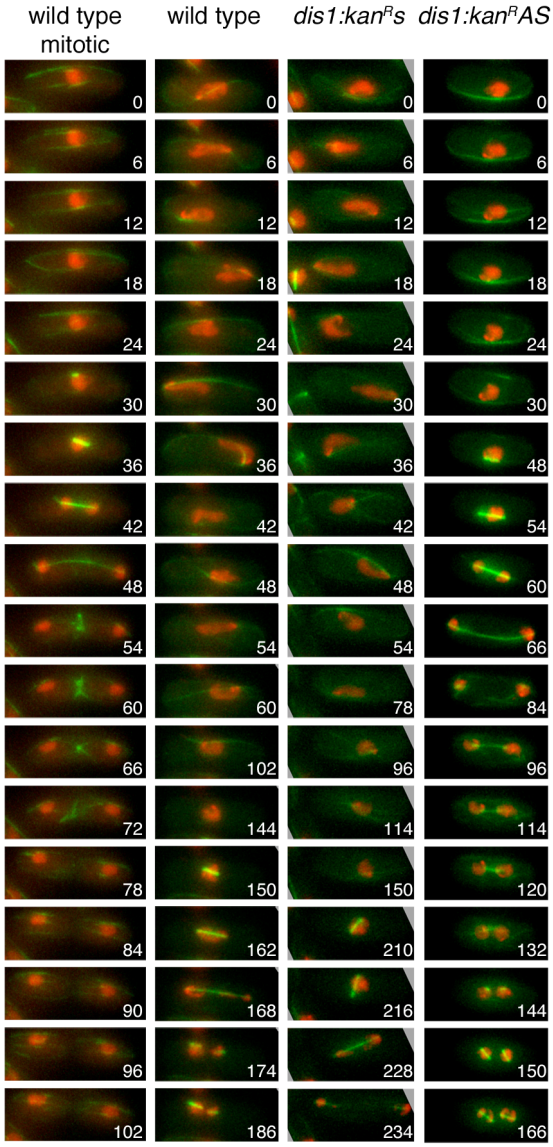

Supplementary Figure S1. Live cell imaging of strains IH10191, IH10192 and IH10110 stained with 10 µg/µl Hoescht 33342.
Cells were grown in EMM2 at 25°C and shifted to 32°C one hour before imaging to induce meiosis. Note the prominent extension and bending of the "horsetail" nuclei in the panels of wild type (12 to 60 minutes), *dis1.kan^{R}s* (6 – 96) while the nucleus in *dis1.kan^{R}AS* resembled that of the wild type mitotic samples over the equivalent period; the nucleus did not adopt the "horsetail" configuration.

Supplementary Table S1. Distribution of TBlocks when positioned against standard and augmented *S. pombe* annotation

Classification	Range of TBlocks (bp)	No. of TBlocks 76,315	Number of extended GeneDB accessions
Exonic	50-2,041	27,387	N/A
Extending Exons	50-3,958	9,805	(7,619/10,677) = 71.4%
Intronic	50-276	601	NA
Intergenic	50-919	38,522	NA
Within genes	50-2,041	30,633	NA
Extending genes	50-3,958	7,160	(4,736/5,857) = 80.9%
Distribution of TBlocks when UTR boundaries were used in both orientations			
Genes	50-2795	37,005	NA
Extending Genes	105-1,337	35	NA
Intergenic	50-884	19,931	NA
Antisense	50-1,521	17,898	NA
Extending Antisense	50-3,958	1,446	
Number of TBlocks after splitting extensions in both orientations			
Genes	1-2,795	37,040	NA
Intergenic	1-884	21,199	NA
Antisense	1-1,521	19,344	NA

Supplementary Table S3. The number and type of genomic regions interrogated

Classification	Number of regions	Regions with sequence reads in at least one sample
Annotated genes	5,857	5,459
Antisense loci	5,857	4,384
Introns	4,825	2,322
Intergenic	21,199	20,726
Total	37,738	32,891

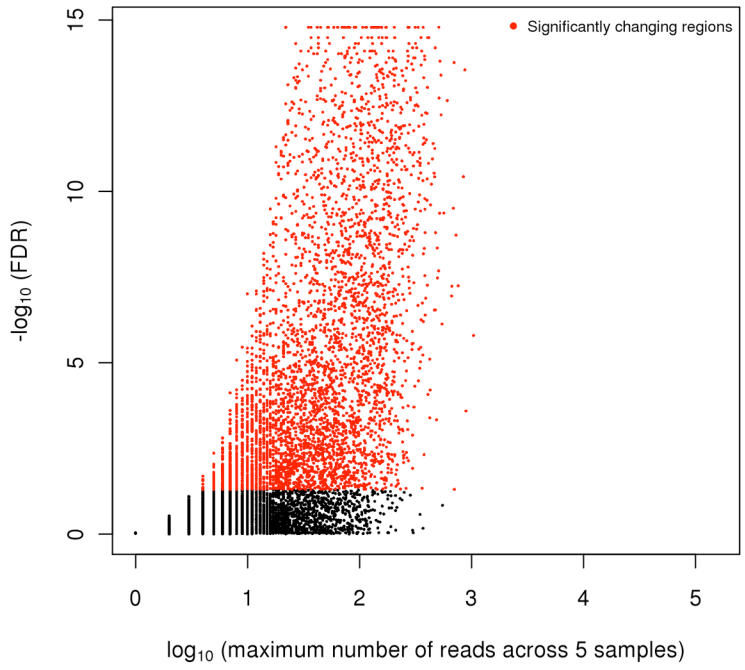

Supplementary Figure S2. *S. pombe* regions with altered transcript levels (FDR < 0.05) as determined by a G-test applied to RNA sequencing count data.
Sequence reads were obtained for five samples as follows: asynchronous haploid wild type (*972* h$^-$), *pat1.114/ pat1.114* diploid in mid log phase vegetative growth (0 hours) and at three timepoints during a temperature induced meiosis (3, 5 and 10 hours). In total, 32,891 genomic regions were interrogated (black), while 6,599 where found to be changing in at least one sample (red).

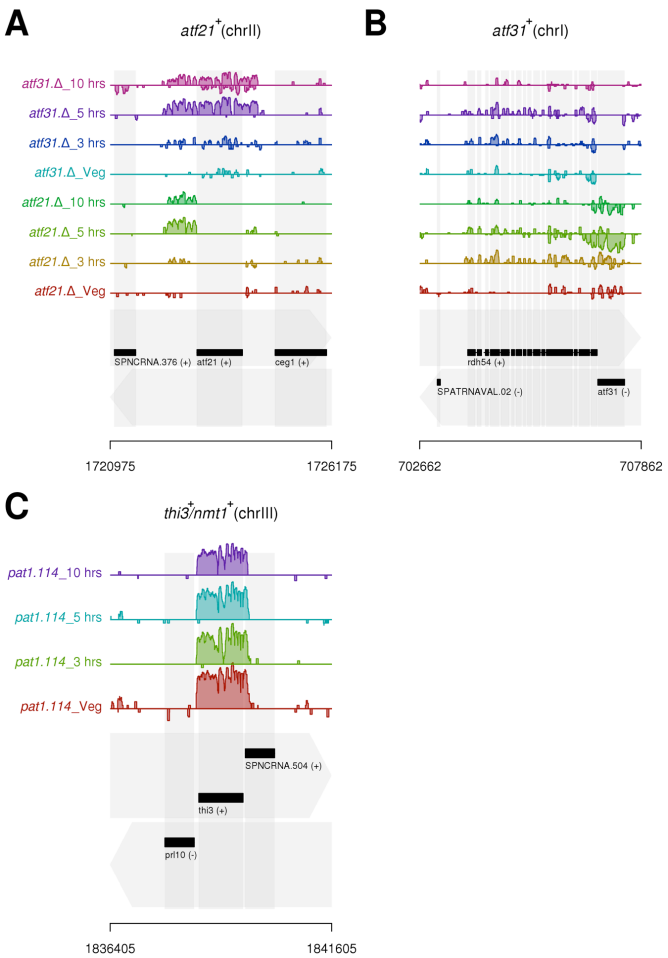

Supplementary Figure S3. Transcript abundance of *atf21*$^+$, *atf31*$^+$ and *thi3*$^+$/*nmt1*$^+$ loci in *atf21*.Δ, *atf31*.Δ and vegetative *pat1.114/ pat1.114* wild type diploid and synchronised meiotic datasets.

Selected parts of the *S. pombe* genome. Genome annotation is indicated in the bottom of each panel, with top and bottom strand indicated by the grey arrows in the background. Exons are shown by black rectangles, with direction of transcription indicated by (+) or (-). Normalised, strand-specific, RNA sequencing data on a $\log_2$ scale are presented in the tracks above, with forward-strand transcription shown above the centre-line of each track, reverse-strand transcription, below. All strains are diploids that are homozygous for both *pat1.114* and the *atf* allele. Each track represents a different sample, as indicated. (**A**) *atf21*$^+$ expression profiles in *atf31*.Δ and *atf21*.Δ datasets. Fold changes for *atf21*$^+$ were significant at vegetative state ($\log_2$ fold change: 24.3; FDR $< 3.19\times10^{-12}$), and at timepoint 3 hrs (Fold change: 4.1; FDR $< 1.15\times10^{-7}$) in the absence of *atf31*$^+$ (*atf31*.**Δ**) compared to the equivalent samples in the wild type control dataset. (**B**) *atf31*$^+$ expression profiles in *atf21*.Δ and *atf31*.Δ datasets. $\log_2$ fold changes for *atf31*$^+$ were significant at timepoint 5 hrs ($\log_2$ fold change: 0.46; FDR $<1.12\times10^{-5}$), and at timepoint 10 hrs ($\log_2$ fold-change: 3.7; FDR ~0) in the absence of *atf21*$^+$ (*atf21*.**Δ**) compared to the equivalent sample in *pat1.114/pat1.114 atf21*$^+$/*atf21*$^+$dataset. (**C**) *nmt1*$^+$ (*thi3*$^+$) expression profile in *pat1.114/pat1.114 atf21*$^+$/*atf21* dataset.

Supplementary Table S8. The number of sequence reads obtained for each sample. mm: mismatches; Veg: Vegetative growth.

Run	Sample	Unique reads (3mm)	Unique junction reads (3mm)	Non-unique reads (0mm)	Unique reads (0mm)	Unique junction reads (0mm)
1st	Haploid Veg (*972* h-)	2,454,972	37,894	3,458,848	679,672	10,502
	*pat1.114*_Veg (diploid ,time 0)	6,596,564	66,048	10,760,215	1,861,613	19,173
	*pat1.114*_3_hr	2,627,403	28,454	3,925,107	727,910	8,231
	*pat1.114*_5_hr	2,970,532	35,457	3,886,259	775,966	10,003
	*pat1.114*_10_hr	3,631,419	28,224	4,661,029	924,748	8,390
2nd	diploid Veg	5,248,386	71,752	10,463,396	1,538,496	20,213
	Haploid Veg (*972* h-)	5,326,784	64,851	14,512,104	1,607,067	19,486
	*pat1.114*_Veg (diploid ,time 0)	6,784,746	93,167	9,502,115	1,979,004	26,241
	*pat1.114*_3_hr	2,198,240	28,604	6,250,166	614,608	8,061
	*pat1.114*_5_hr	4,083,167	47,553	6,708,683	1,128,778	14,009
	*pat1.114*_10_hr	2,493,572	21,311	9,523,194	684,390	6,300
	atf21.Δ_ *pat1.114*_Veg (diploid ,time 0)	7,004,364	95,520	10,065,794	2,080,901	27,056
	atf21.Δ _ *pat1.114*_3_hr	4,818,515	64,421	6,822,336	1,404,529	19,272
	atf21.Δ _ *pat1.114*_5_hr	3,319,073	40,039	5,161,295	969,010	12,532
	atf21.Δ _ *pat1.114*_10_hr	1,320,520	11,438	7,171,624	373,242	3,468
	atf31.Δ _ *pat1.114*_Veg (diploid ,time 0)	3,642,404	52,269	8,693,897	1,084,952	15,361
	atf31.Δ_ *pat1.114*_3_hr	3,488,205	48,800	7,199,376	1,046,936	15,031
	atf31.Δ _ *pat1.114*_5_hr	6,139,379	78,085	8,895,405	1,787,263	24,514
	atf31.Δ _ *pat1.114*_10_hr	3,438,982	26,006	9,551,539	949,806	8,156

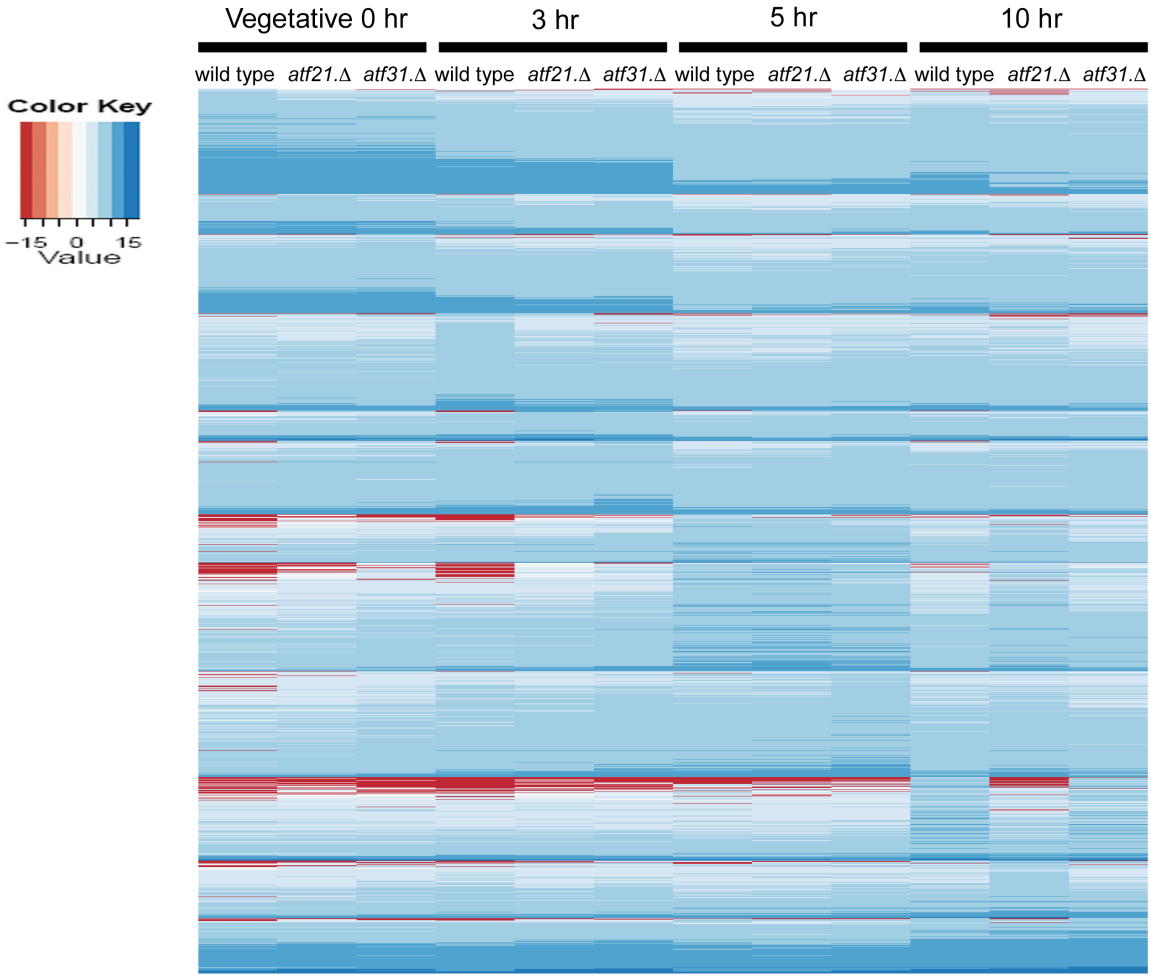

Supplementary Figure S4. Expression profiles of 1,714 regions with significant changes in transcript level between *atf21*.Δ or *atf31*.Δ mutant and the wild type control strains.

Heatmap showing the expression patterns of statistically significant regions that were found to be changing in at least one sample. Differential expression was determined using count data and a Fisher exact test as described in (Bloom et al, 2009). In brief, a series of pair-wise comparisons were conducted in order to compare the read counts of each gene at a given sample between wild type (*pat1.114*) cells and each of the mutant strains (*pat1.114 atf21*.Δ or *pat1.114 atf31*.Δ). All strains are diploids that are homozygous for both *pat1.114* and the *atf* allele. P-values were adjusted to account for multiple testing and a FDR computed. A threshold of < 0.0125 was applied. Transcript levels were normalized both by the total number of reads within a sample and by the length of each defined region. Data presented are $\log_2$. Expression data were grouped according to the sample in which a given locus displayed the highest expression level. The 1,714 regions were allocated to the following groups, protein-coding genes (1,332), intronic regions (8), pseudogenes (4), annotated ncRNAs (88), TBlocks (197) and antisense loci (85). Expression values ($\log_2$) colour key (top left).

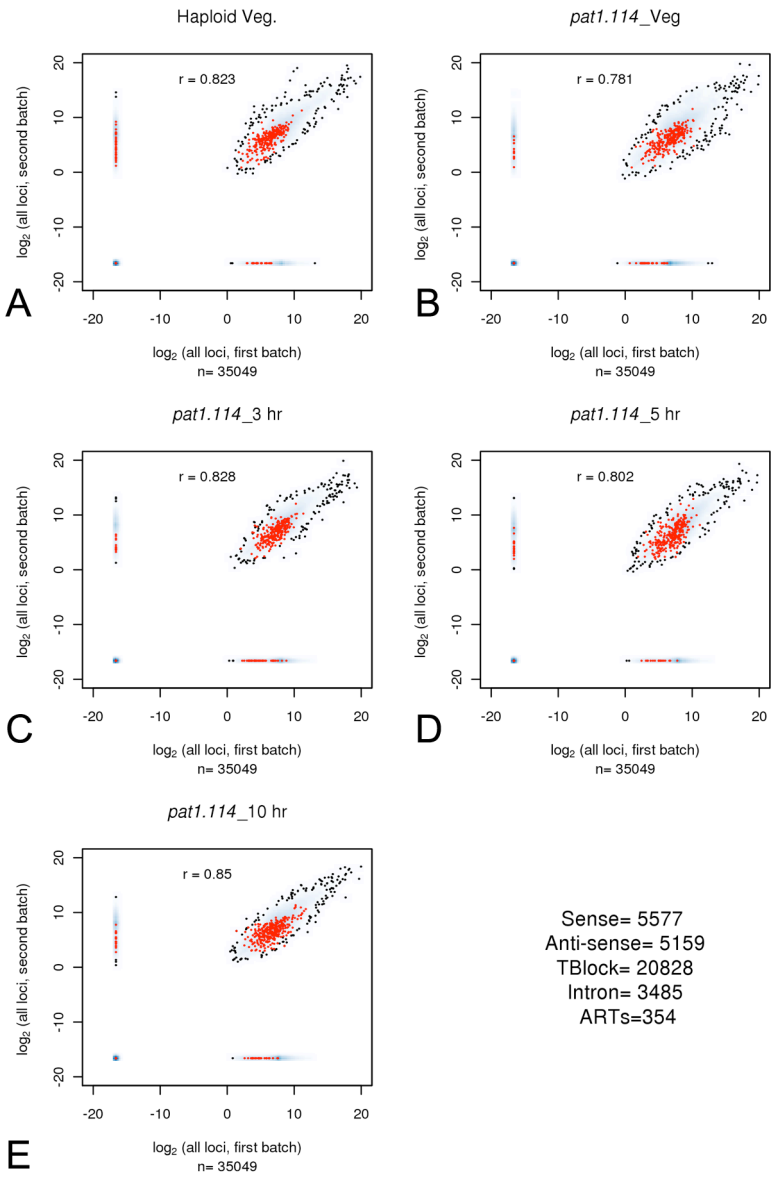

Supplementary Figure S5. Reproducibility of RNA-sequencing data generated in two independent experiments.

Only loci with at least 1 read in any of the 19 samples were interrogated (35049 loci). Sample specific transcript levels for each locus were calculated using RNA sequencing count data generated from two biological replicates, as follows: *972* h^- vegetative haploid (**A**), *pat1.114/pat1.114* diploids in vegetative growth (**B**; 0 hrs) and a *pat1.114/pat1.114* diploid 3 (**C**), 5 (**D**) and 10 hours (**E**) following the temperature shift (first sequencing run: x-axis; second sequencing run; y-axis). Expression values (log_2) were normalized both by the total number of reads within a given sample and by the length of each defined region. Outliers are shown in black; Antisense Regulatory Transcripts (ARTs) in red. Pearson's correlation coefficient ('r') of the main cloud (only those loci with at least 1 read in both the first and second machine runs) are indicated in each panel.

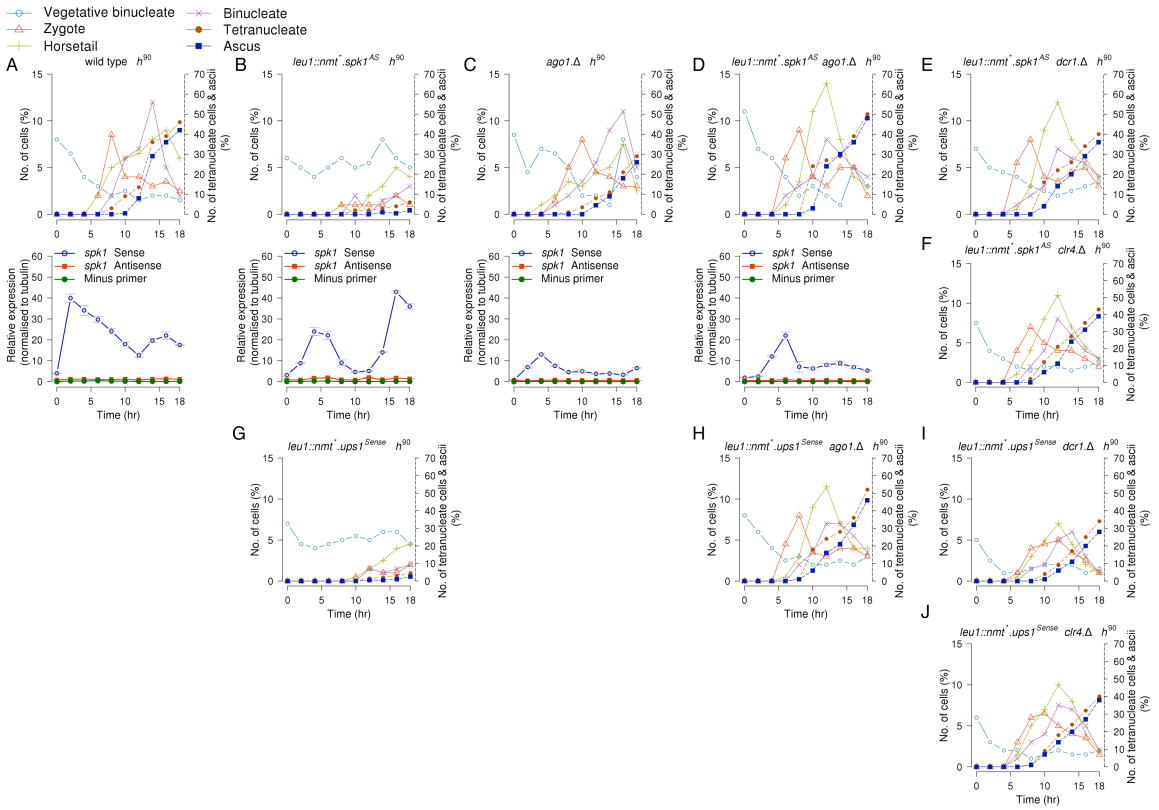

Supplementary Figure S6. Meiotic progression of wild-type, RNAi deleted background and *spk1*^{AS} expressing strains alongside relative qPCR expression levels of *spk1* sense and antisense transcripts.

A, C) Cells of the indicated strains were grown in supplemented EMM2 (which contains 5 gl^{-1} NH_4Cl) for 18 hours to mid log phase before filtration and re-suspension in MSL lacking any nitrogen source at time 0. Samples were taken for DAPI staining to reveal the chromatin configuration and so score meiotic progression (upper panels) and to extract RNA for the strand specific qPCR (lower panels) every two hours as indicated. For panels B, D-J in which antisense transcript expression at the heterologous *leu1* locus was induced by removal of thiamine, cells were grown to mid-log phase in supplemented EMM2 containing 2 μM thiamine before isolation via centrifugation followed by three washes in supplemented EMM2 lacking this vitamin. After a 15 minute incubation in thiamine free medium cells were subject to a final wash and re-suspension in fresh thiamine free medium. Over the next 72 hours the culture density was maintained in low to mid-log phase by dilution before following the nitrogen starvation procedure with a mid – log phase culture as described for panels A and C.

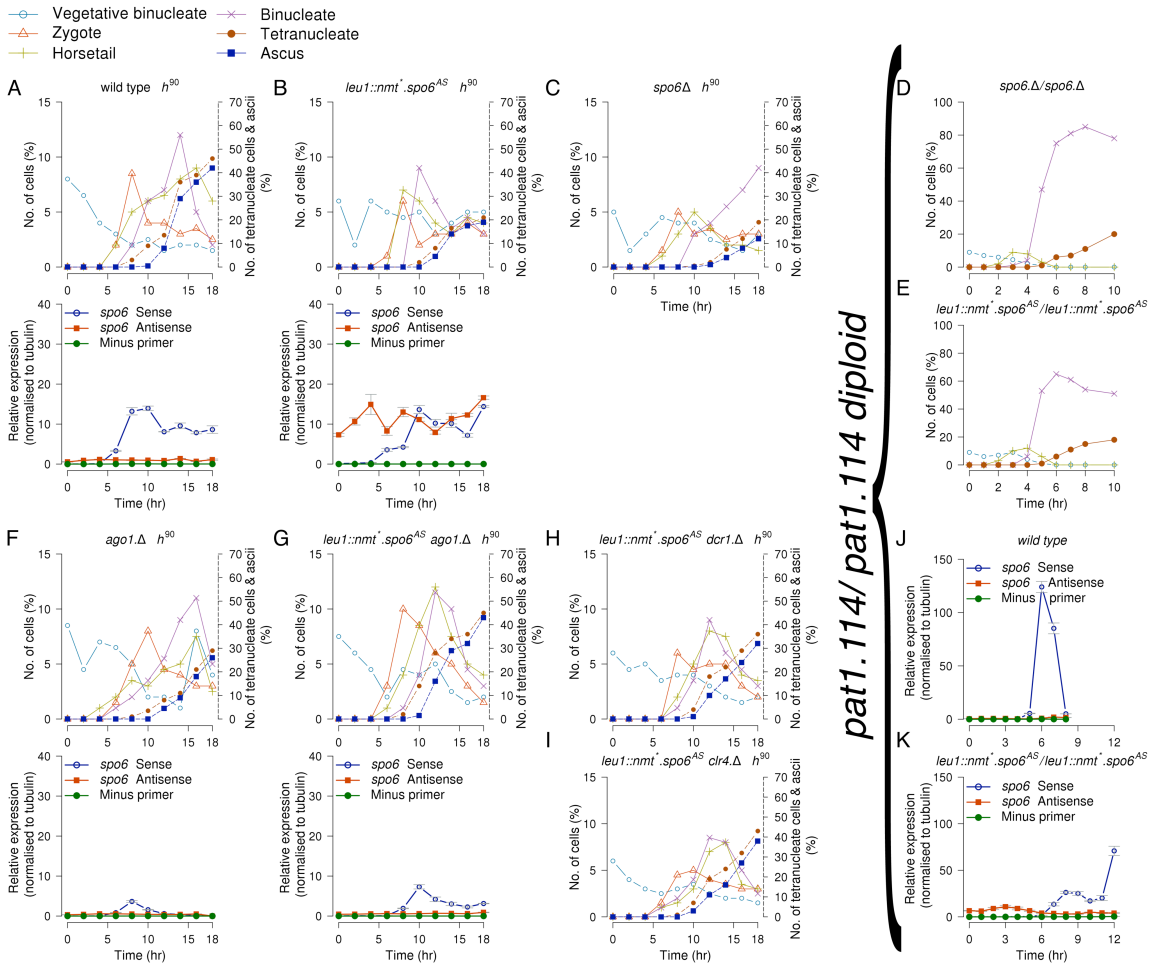

Supplementary Figure S7. Meiotic progression of wild-type, RNAi deleted background and *spo6*^{AS} expressing strains alongside relative qPCR expression levels of *spo6* sense and antisense transcripts.

For the h^{90} strains in panels A-C and F-I growth and induction conditions were as described in the legend to Supplementary Figure S6. For panels D and J cells were grown at 25°C in supplemented EMM2 to mid-log phase before the temperature was shifted to 32°C at time 0 to induce meiotic commitment. Samples were taken for DAPI staining to reveal the chromatin configuration and so score meiotic progression (D, E) and to extract RNA for the strand specific qPCR (J, K) at the indicated intervals. For panels E and K in which antisense transcript expression at the heterologous *leu1* locus was induced by removal of thiamine, cells were grown to mid-log phase at 25°C in EMM2 containing 75 mg ml^{-1} leucine and 2 μM thiamine before isolation via centrifugation followed by three washes in EMM2 + leucine (EMM2L). After a 15 minute incubation in thiamine free EMM2L medium cells were subject to a final wash and re-suspension in fresh thiamine free EMM2L medium. Over the next 72 hours the culture density was maintained in low to mid-log phase by dilution before the temperature was shifted from 25°C to 32°C to induce meiotic commitment. The strains in panels A-C and F-I are all haploid, while those in D, E, J and K are diploid strains that are homozygous for the indicated mutant alleles.

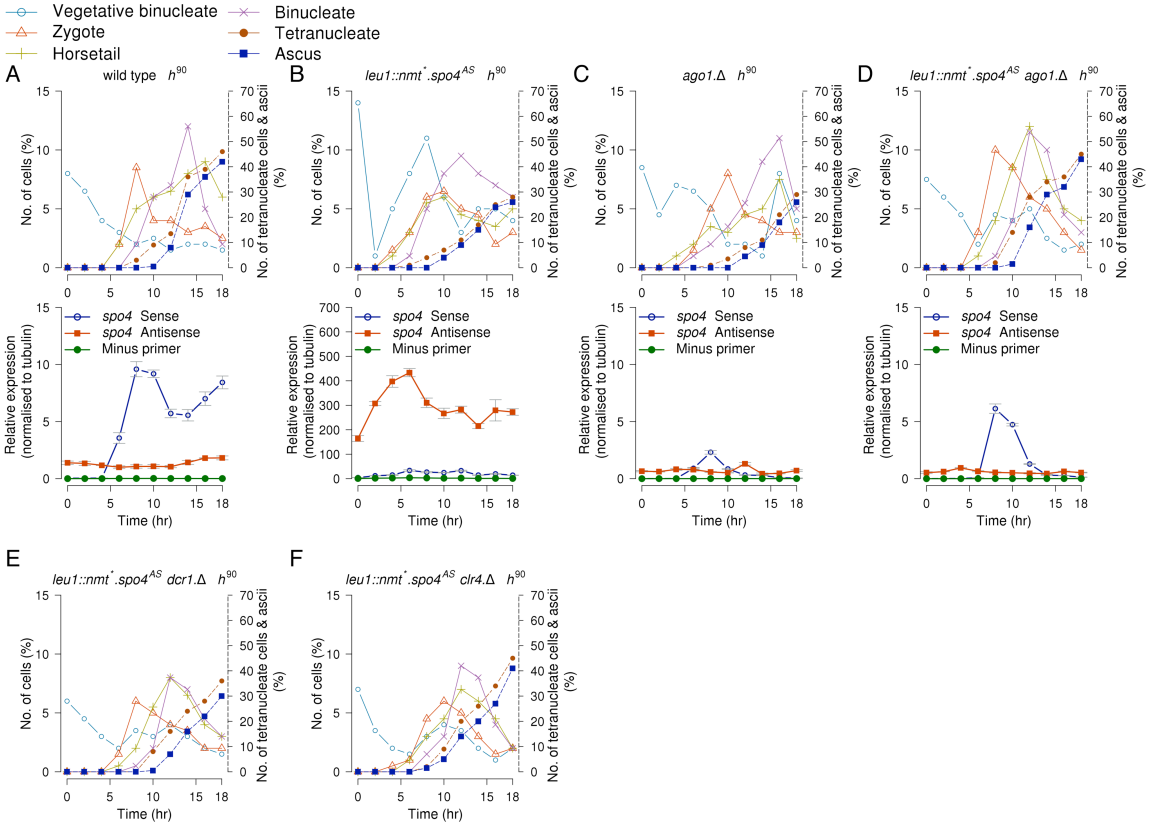

Supplementary Figure S8. Meiotic progression of wild-type, RNAi deleted background and *spo4*^{AS} expressing strains alongside relative qPCR expression levels of *spo4* sense and antisense transcripts.

Growth and induction conditions were as described in the legend to Supplementary Figure S6. All strains characterized in this figure are haploid.

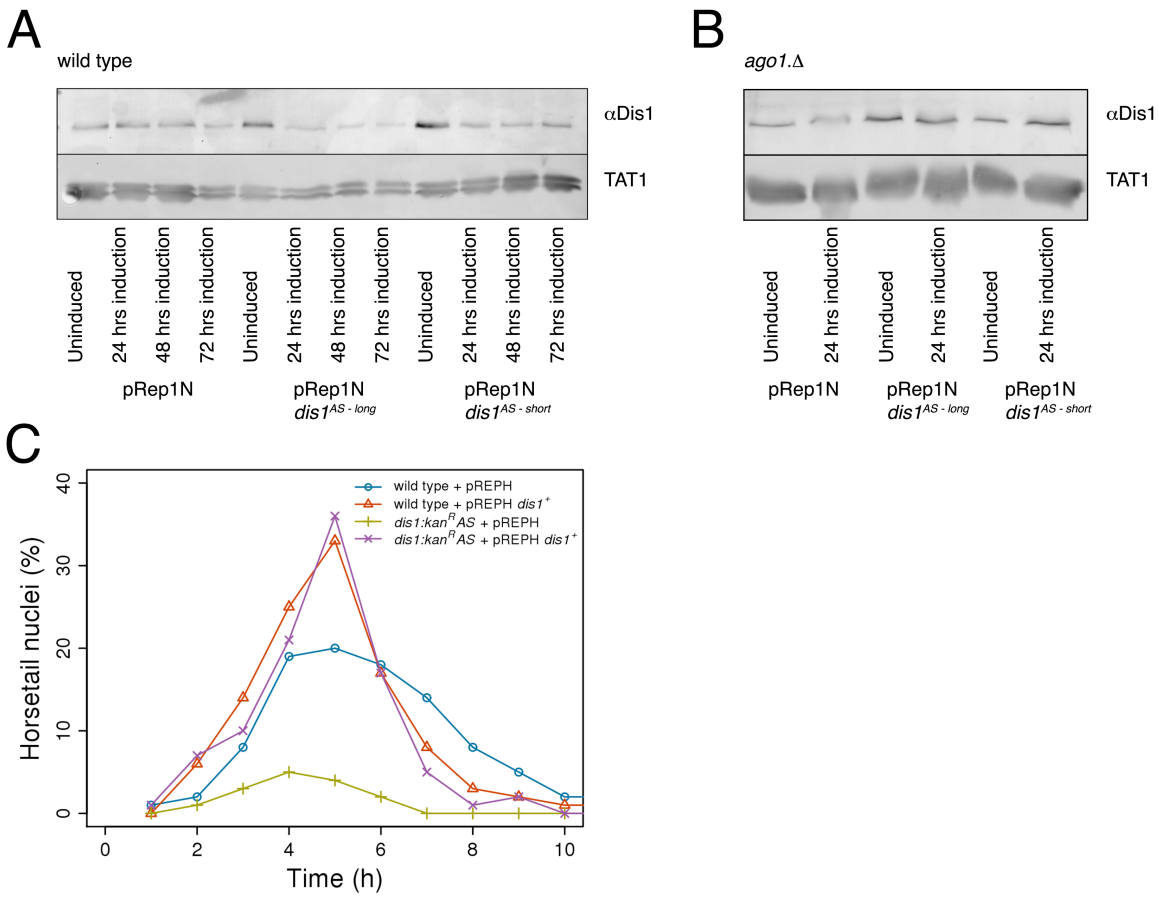

Supplementary Figure S9. Expression of antisense *dis1*$^{+}$ transcripts impacts upon protein levels.

(**A, B**) *972* h^{-} (IH5974) wild type or *ago1::kan*^{R} (IH9677) strains bearing the pRep1N plasmids in which cells have been maintained in log phase for the duration of the study and the *nmt1*$^{+}$ promoter has been de-repressed for the times indicated in the legend below the immunoblots to detect the indicated proteins. (**B)** A repeat of the approach in **A** using an *ago1::kan*^{R} background instead. (**C**) The indicated strains (mating type h^{90}) were grown to mid-log phase in medium containing thiamine, before being washed three times in medium lacking thiamine to induce transcription from the *nmt1*$^{+}$ promoter on the pREPH vectors. 48 hours later cells were subjected to nitrogen starvation and the frequency of horsetail movement assessed by anti-tubulin immunofluorescence and DAPI staining.

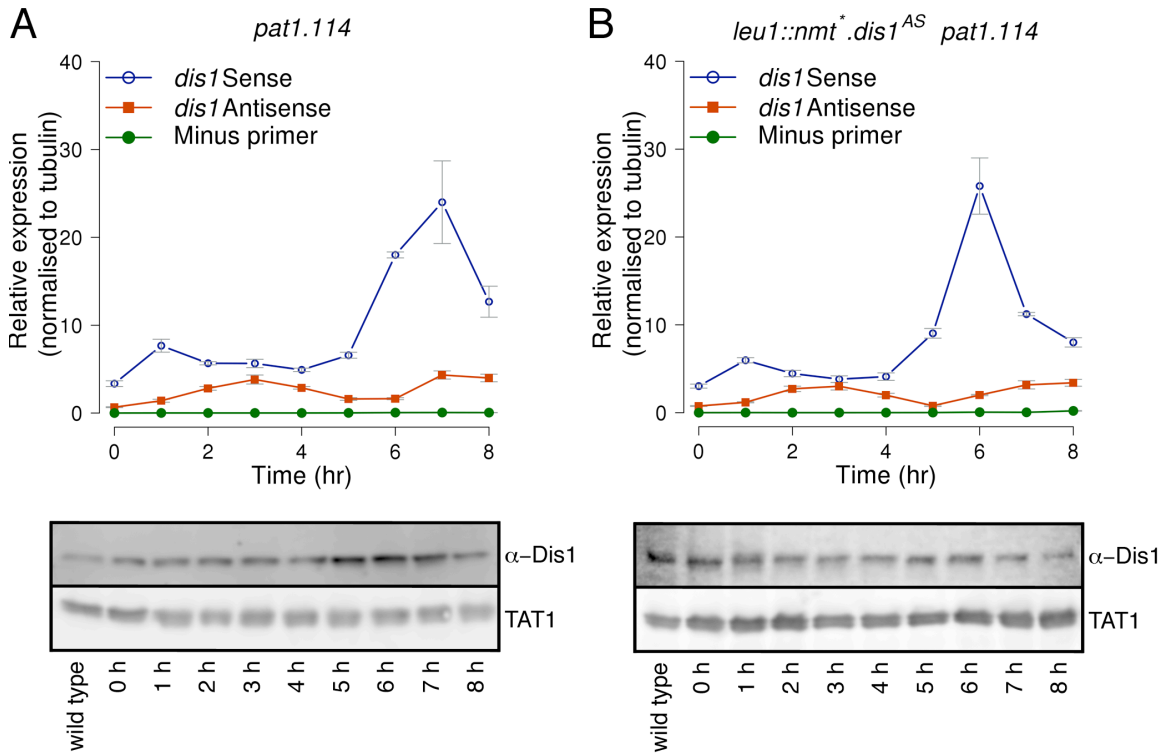

Supplementary Figure S10. Meiotic progression of wild-type, RNAi deleted background and *dis1*^{AS} expressing in *pat1.114* diploid strains.
A) Diploid cells homozygous for *pat1.114* mutation were grown at 25°C in supplemented EMM2 to mid-log phase before the temperature was shifted to 32°C at time 0 to induce meiotic commitment. Samples were taken for DAPI staining to reveal the chromatin configuration and so score meiotic progression and to prepare protein extracts every two hours after the shift. Western blots of the SDS PAGE gels of the extracts were cut into two and probed with antibodies to either Dis1 (upper) or α-tubulin (TAT1 – lower). B) *leu1::nmt*.dis1*^{AS} *pat1.114* cells were grown to mid-log phase at 25°C in EMM2 containing 75 mg ml^{-1} leucine and 2 μM thiamine before isolation via centrifugation followed by three washes in EMM2 + leucine (EMM2L). After a 15 minute incubation in thiamine free EMM2L medium cells were subject to a final wash and re-suspension in fresh thiamine free EMM2L medium. Over the next 48 hours the culture density was maintained in low to mid-log phase by dilution before the temperature was shifted from 25°C to 32°C to induce meiotic commitment.

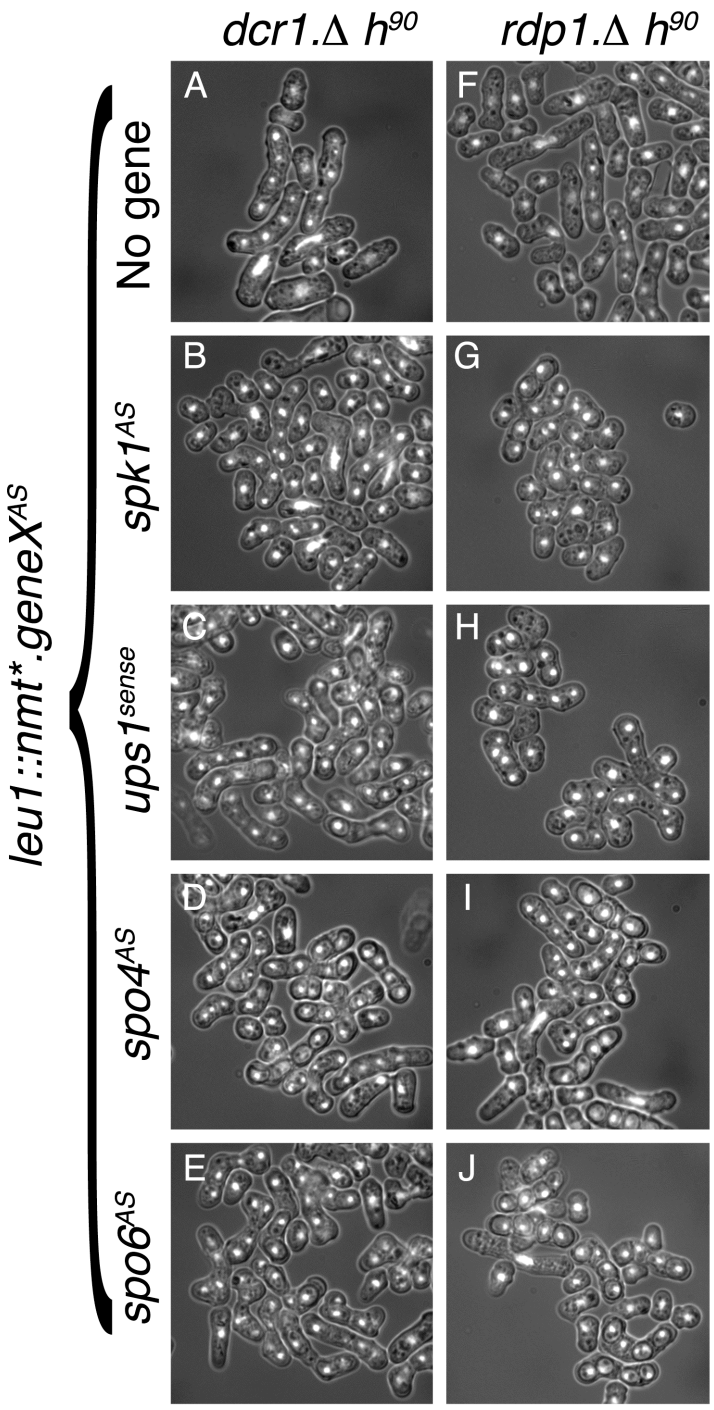

Supplementary Figure S11. Antisense RNA production perturbs Spk1 and Spo4/Spo6 function in Dcr1 and Rdp1 dependent manner.

The indicated strains processed as described for Figure 6 A-J.

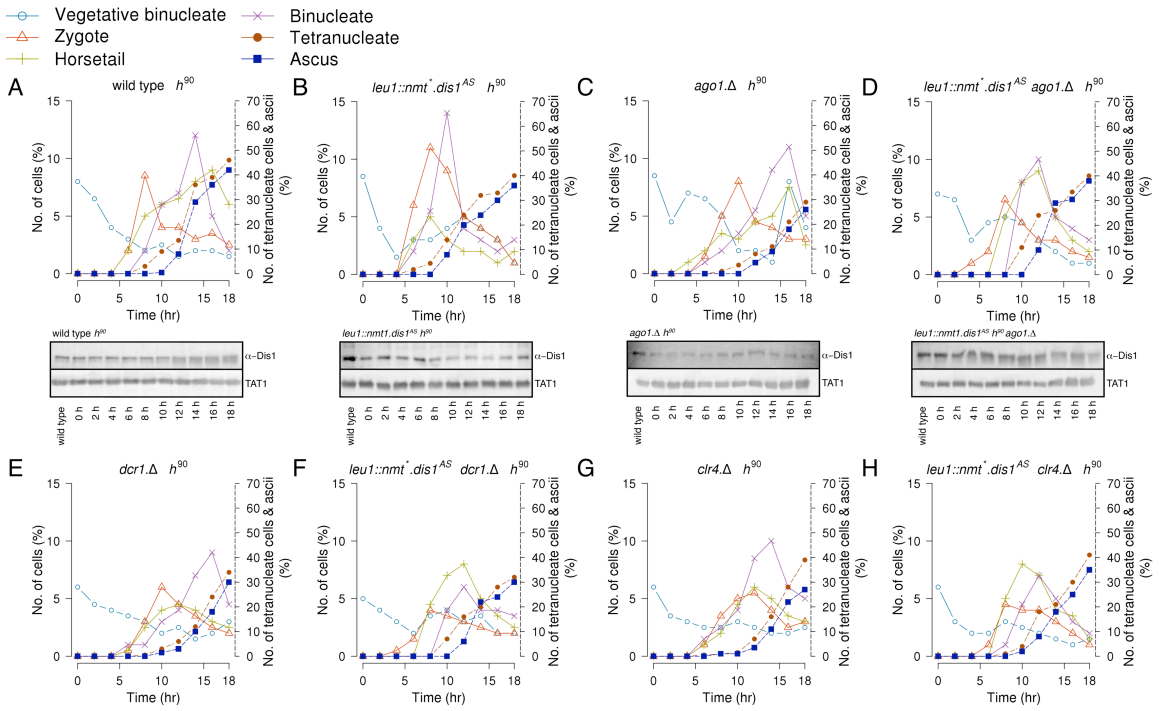

Supplementary Figure S12. Meiotic progression of wild-type, RNAi deleted background and dis1^{AS} expressing h^{90} strains.

Growth and induction conditions were as described in the legend to Supplementary Figure S6. All strains characterized in this figure are haploid. For panels A-D protein extracts were prepared every two hours subject to SDS PAGE followed by Western blotting. The blots were cut into two and probed with antibodies to either Dis1 (upper) or α-tubulin (TAT1 – lower).

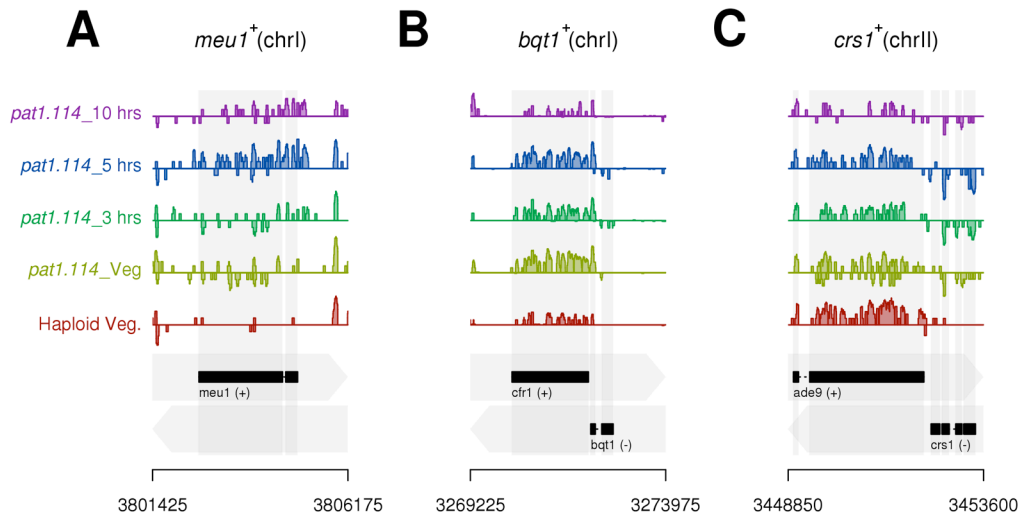

Supplementary Figure S13. Transcript profiles of *meu1*$^+$, *bqt1*$^+$ and *crs1*$^+$ loci in haploid at vegetative growth and *pat1.114* at vegetative growth (0) and at 3, 5 and 10 hours following temperature shift

Selected parts of the *S. pombe* genome. Genome annotation is indicated in the bottom of each panel, with top and bottom strand indicated by the grey arrows in the background. Exons are shown by black rectangles, with direction of transcription indicated by (+) or (-). Normalised, strand-specific, RNA sequencing data on a $\log_2$ scale are presented in the tracks above, with forward-strand transcription shown above the centre-line of each track, reverse-strand transcription, below. Each track represents a different sample, as indicated. (**A**) *meu1*$^+$ (**B**) *bqt1*$^+$ and (**C**) *crs1*$^+$ expression profiles in both orientations in *pat1.114/ pat1.114* diploid dataset. Colours represent expression data originating from different samples as indicated in the legend (left).

Supplementary Table S11. *S. pombe* strains used in this study

Strain Number	Genotype	Source
IH180	*h⁻ pat1.114*	Lab Stock
IH347	h^{90}	Lab Stock
IH2912	*h⁻/h⁺ pat1.114/pat1.114 ade6.M210/ade6.M216*	Lab Stock
IH3365	*h⁻/h⁺ ade6.M210/ade6.M216*	Lab Stock
IH5974	h⁻ *972*	Lab Stock
IH8794	*h⁺ rpl42::cyhR.SP56Q leu1.32 ura4.d18*	Roguev *et al.* (2007) *Nat Methods* **4:** 861-866
IH8814	*h⁻/h⁺ pat1.114/pat1.114 ade6.M210/ade6.M216 atf31::kan^{R}MX6/atf31::kan^{R}MX6*	This study
IH8832	*h⁻/h⁺ pat1.114/pat1.114 ade6.M210/ade6.M216 atf21::natMX6/atf21::natMX6*	This study
IH8833	*h⁻/h⁺ pat1.114/pat1.114 ade6.M210/ade6.M216 spo6::kan^{R}MX6/spo6::kan^{R}MX6*	This study
IH9675	*h⁻/h⁺ pat1.114/pat1.114 ade6.M210/ade6.M216 dis1.kan^{R}AS/dis1.kan^{R}AS*	This study
IH9677	*h^{90} ago1::kan^R*	Volpe *et al.* (2002) *Science* **297**: 1833-1837
IH9748	*h^{90} spo6::kan^{R}MX6*	This study
IH9758	*h⁻/h⁺ pat1.114/pat1.114 ade6.M210/ade6.M216 dis1.kan^{R}s/dis1.kan^{R}s*	This study
IH9985	*h^{90} clr4::natMX6 ura4.d18 leu1.32*	Bayne *et al.* (2010) *Cell* 1**40**: 666-677
IH9987	*h^{90} dcr1::natMX6 ura4.d18 leu1.32 his3.d1*	Provost *et al.* (2002) *PNAS* **99:**16648-16653
IH9989	*h^{90} rdp1::natMX6 ura4.d18 leu1.32*	Volpe .*et al* (2003) *Chromosome Res*. **11:**137-146
IH9991	*h⁻ dis1::ura4⁺ ura4.d18 leu1.32*	Nabeshima *et al.* (1995) *Genes Dev* **9:**1572-1585
IH9999	*h⁻ leu1::nmt*dis1.AS:ura4⁺ ura4.d18*	This study
IH10000	*h^{90} leu1::nmt*spo4.AS:ura4⁺ ura4.d18*	This study
IH10005	*h^{90} leu1::nmt*spo6.AS:ura4⁺ ura4.d18*	This study
IH10006	*h^{90} leu1::nmt*ups1:ura4⁺ ura4.d18*	This study
IH10043	*h⁻ ago1::kan^R leu1::nmt*dis1.AS:ura4⁺ ura4.d18*	This study
IH10044	*h^{90} ago1::kan^R leu1::nmt*dis1.AS:ura4⁺ ura4.d18*	This study
IH10045	*h⁻ dcr1::natMX6 leu1::nmt*dis1.AS:ura4⁺ ura4.d18*	This study
IH10046	*h^{90} dcr1::natMX6 leu1::nmt*dis1.AS:ura4⁺ ura4.d18*	This study
IH10047	*h⁻ rdp1::natMX6 leu1::nmt*dis1.AS:ura4⁺ ura4.d18*	This study
IH10048	*h^{90} rdp1::natMX6 leu1::nmt*dis1.AS:ura4⁺ ura4.d18*	This study
IH10051	*h^{90} ago1::kan^R leu1::nmt*spo4.AS:ura4⁺ ura4.d18*	This study
IH10054	*h^{90} rdp1::natMX6 leu1::nmt*spo4.AS:ura4⁺ ura4.d18*	This study
IH10056	*h^{90} ago1::kan^R leu1::nmt*spo6.AS:ura4⁺ ura4.d18*	This study
IH10058	*h^{90} dcr1::natMX6 leu1::nmt*spo6.AS:ura4⁺ ura4.d18*	This study

IH10060	*h^{90} rdp1::natMX6 leu1::nmt*spo6.AS:ura4^{+} ura4.d18*	This study
IH10061	*h^{90} leu1::nmt*spk1.AS:ura4^{+} ura4.d18*	This study
IH10063	*h^{90} ago1::kan^{R} leu1::nmt*spk1.AS:ura4^{+} ura4.d18*	This study
IH10067	*h^{90} dcr1::natMX6 leu1::nmt*spk1.AS:ura4^{+} ura4.d18*	This study
IH10070	*h^{90} ago1::kan^{R} leu1::nmt*ups1:ura4^{+} ura4.d18*	This study
IH10072	*h^{90} dcr1::natMX6 leu1::nmt*ups1:ura4^{+} ura4.d18*	This study
IH10101	*h^{90} dcr1::natMX6 leu1::nmt*spo4.AS:ura4^{+} ura4.d18*	This study
IH10102	*h^{-} clr4::natMX6 leu1::nmt*dis1.AS:ura4^{+} ura4.d18*	This study
IH10103	*h^{90} clr4::natMX6 leu1::nmt*dis1.AS:ura4^{+} ura4.d18*	This study
IH10105	*h^{90} rdp1::natMX6 leu1::nmt*spk1.AS:ura4^{+} ura4.d18*	This study
IH10107	*h^{90} atf21::natMX6*	This study
IH10108	*h^{90} atf31::kan^{R}MX6*	This study
IH10110	*h^{-}/h^{+} pat1.114/pat1.114 ade6.M210/ade6.M216 leu1::nmt*dis1.AS:ura4^{+}/leu1::nmt*dis1.AS:ura4^{+} ura4.d18/ ura4.d18*	This study
IH10144	*h^{-}/h^{+} dis1::ura4^{+}/dis1::ura4^{+}pat1.114/pat1.114 ade6.M210/ade6.M216 ura4.d18/ ura4.d18*	This study
IH10145	*h^{-}/h^{+} pat1.114/pat1.114 ade6.M210/ade6.M216 dis1.kan^{R}AS/dis1.kan^{R}AS leu1::atb2GFP:ura4^{+}/ leu1::atb2GFP:ura4^{+} ura4.d18/ ura4.d18*	This study
IH10173	*h^{90} rdp1::natMX6 leu1::nmt*ups1:ura4^{+} ura4.d18*	This study
IH10191	*h^{-}/h^{+} pat1.114/pat1.114 ade6.M210/ade6.M216 leu1::atb2GFP:ura4^{+}/ leu1::atb2GFP:ura4^{+} ura4.d18/ ura4.d18*	This study
IH10192	*h^{-}/h^{+} pat1.114/pat1.114 ade6.M210/ade6.M216 dis1.kan^{R}s/dis1.kan^{R}s leu1::atb2GFP:ura4^{+}/ leu1::atb2GFP:ura4^{+} ura4.d18/ ura4.d18*	This study
IH9778	*spo6::kanMX6/spo6::kanMX6 pat1.114/pat1.114 ade6.M210/ade6.M216 h^{-}/h^{+}*	This study
IH10444	*pat1.114/pat1.114 ade6.M210/ade6.M216 leu1::nmt*spo6^{AS}:ura4^{+}/leu1::nmt*spo6^{AS}:ura4^{+} ura4.d18/ura4.d18 h^{-}/h^{+}*	This study